Dynamic Mode Decomposition for Large-Scale Coherent Structure Extraction in Shear Flows

Duong B. Nguyen, Panruo Wu, Rodolfo Ostilla Monico, Guoning Chen, *Member, IEEE,*

Abstract—Large-scale structures have been observed in many shear flows which are the fluid generated between two surfaces moving with different velocity. A better understanding of the physics of the structures (especially large-scale structures) in shear flows will help explain a diverse range of physical phenomena and improve our capability of modeling more complex turbulence flows. Many efforts have been made in order to capture such structures; however, conventional methods have their limitations, such as arbitrariness in parameter choice or specificity to certain setups. To address this challenge, we propose to use Multi-Resolution Dynamic Mode Decomposition (mrDMD), for large-scale structure extraction in shear flows. In particular, we show that the slow motion DMD modes are able to reveal large-scale structures in shear flows that also have slow dynamics. In most cases, we find that the slowest DMD mode and its reconstructed flow can sufficiently capture the large-scale dynamics in the shear flows, which leads to a parameter-free strategy for large-scale structure extraction. Effective visualization of the large-scale structures can then be produced with the aid of the slowest DMD mode. To speed up the computation of mrDMD, we provide a fast GPU-based implementation. We also apply our method to some non-shear flows that need not behave quasi-linearly to demonstrate the limitation of our strategy of using the slowest DMD mode. For non-shear flows, we show that multiple modes from different levels of mrDMD may be needed to sufficiently characterize the flow behavior.

Index Terms—Flow visualization, Shear Flows, Dynamic Mode Decomposition

1 Introduction

Turbulent flows are often characterized by chaotic motion and random mixing. Understanding turbulent flows is a critical task for the success of many different fields in science and industry such as automobile and aircraft engineering, climate study, combustion dynamics, and medicine. A very relevant type of turbulent flow is *wall-bounded shear flows*, which are generated in a fluid between two surfaces with different velocities. These have been extensively used to explore new concepts in fluid mechanics such as instabilities [50], non-linear hydrodynamics [49], and pattern formation [4]. Two popular wall-bounded shear flows are plane Couette flow [29] and Waleffe flow [9]. The former is the flow between two infinite plates which move with different velocities, while the latter is the flow bounded by two infinite stress-free plates and forced using a body shear forcing force.

The nature of turbulence involves a process where energy and other quantities are transferred across scales. The detailed mechanics enabling this transfer are still not well-understood. To understand that, coherent structures at different (time- and length-) scales need to be identified. We can characterize the difference between the small- and large- scale structures based on their size and movement. As the names imply, small structures have smaller sizes and faster time-scales. On the other hand, the large-scale structures are bigger in term of size but have slow dynamics. Large-scale coherent structures are often responsible for the lion's share of the transport of mass, heat and momentum in flows, while small-scale structures are often responsible for energy dissipation [42]. They are tightly coupled: large-scale structures modulate the appearance of small-scale structures, and can act as transport barriers, thus, identifying large-scale structures is often the first and an important step in turbulence study.

Large-scale structures have been observed in shear flows [9], but extracting these structures is not trivial. Many approaches [8], [26], [36], [44] have been developed by the fluid mechanics and the visualization communities to assist experts understand coherent structures and flow dynamics. In fluid mechanics, moving ensemble averages [32], two-point correlations [48], and Fourier analysis [31] have been used to detect and analyze coherent structures. The main disadvantage of these methods is that they often include the relatively arbitrary choice of a cut-off to isolate the structures, be it in the shape of a cut-off frequency in Fourier space [31], or in the shape of a threshold value for a certain attribute [1]. As a result, conventional methods can completely fail to track the structures across certain dimensions of parameter space. Finding a method which requires minimum thresholding remains a challenge.

Dynamic mode decomposition (DMD) is a data-driven and parameter-free method, introduced by Schmidt [46]. It provides a spatio-temporal decomposition of data into a set of relevant dynamical modes called DMD modes from a sequence of snapshots of an evolving system. Each DMD mode is considered as a spatial structure which is accompanied by time dynamics. The corresponding time dynamics of DMD modes can be characterized by their speeds (e.g., how fast or slow they move), making DMD a promising candidate to extract coherent structures (evolving with different speeds) in flow. Several works [58] have attempted to apply DMD to different kinds of flows. For example, Gilka et al. [13] performed a DMD analysis on the flow behind an actuated bluff body, and Schmid [46] tried DMD with the Gurney flap wake flow to capture the vortex shedding pattern. However, the capabilities of DMD in analyzing shear flows have not been fully investigated. In addition, DMD has not received much attention from the visualization community for the task of spatial and

• *Duong B. Nguyen, Panruo Wu, Rodolfo Ostilla Monico, Guoning Chen are with the University of Houston. E-mail: gchen22@central.uh.edu.*

temporal feature extraction.

To fill this gap, in this paper we propose to use Multi-Resolution Dynamic Mode Decomposition (mrDMD) [25], which is a variant of the standard DMD, for large-scale structure extraction in shear flows. Our method is inspired by an intuition about the large-scale structures of shear flows. Although these large structures are hard to extract, it is believe that they behave in a quasi -linear manner [27], [52], making them suitable for DMD analysis. In brevity, the contributions of this work are two-folded. First, we connect the slow motion DMD modes extracted by mrDMD with the large-scale structures in shear flows. In particular, we show that the slowest mode of the first level mrDMD can already sufficiently capture the large-scale structures in the shear flows, allowing us to develop a *parameter-free* large-scale structure extraction technique based on DMD for shear flows. Second, to speed up the computation of mrDMD and enable it to be applicable to large-scale time-dependent 3D turbulent flow data, we provide a fast GPU-based implementation. With this fast mrDMD, large-scale structures of shear flows can be extracted and visualized efficiently. We have applied our method to 2D and 3D Plane Couette (PC) and Waleffe flows using both 2D cuts and full 3D flow fields to demonstrate its effectiveness. This is the first time mrDMD is applied to 3D Plane Couette and Waleffe flow snapshots for large-scale structure extraction.

We compare our DMD based method with other existing methods, such as convolution kernel based smoothing, time average, and the proper orthogonal decomposition (POD) to demonstrate its advantages. In addition, we perform experiments of DMD on other types of flows than shear flows and found that the slowest DMD mode may not always extract useful structures. Instead, modes selected from different levels of mrDMD can better capture the dynamics of those non-shear flows. We report these experiments and attempt to provide some empirical guideline for the visualization community on the proper use of DMD, especially mrDMD, for turbulence flow analysis and visualization.

2 Related Work

In this section, we review the most relevant works in both fluid dynamics and visualization communities for coherent structure extraction and vector field decomposition for turbulent flows.

Coherent structure extraction. Based on the extracted features and attributes, existing approaches for coherent structure extraction can be broadly divided into four categories [14], namely Line-based, Geometry-/Integration-based, Lagrangian-based and Region-based. Line-based techniques [34] try to find the coreline of vortices which are the most important coherent structures. Geometric-based methods [40], [41] focus on constructing the skeleton of a vortex tube. These methods are local. However, it was shown that there are classes of vortices that cannot be extracted by local methods, for instance attracting vortices that move on non-linear paths. As a solution, integration-based methods measuring particle density estimation [56] and analyzing of Jacobian [55] were developed. These methods propose to inject a number of particles and observe their attraction behavior over time.

Lagrangian Coherent structures (LCS) [19], [47], i.e., curves (2D) or surfaces (3D) in the domain across which the flux is negligible, were introduced to identify separation structures in unsteady flow. The computation of LCS was first introduced by Haller [17] by computing the *Finite-Time Lyapunov Exponent (FTLE)*, whose ridges indicate the LCS. FTLE measures the separation of nearby particles given a time interval, and has been compared with the separatrices in the steady case [43], and its computational performance has been substantially improved [11]. There have been numerous studies in the visualization community to investigate and propose visualization frameworks for LCS, such as [10], [11], [15]. The main advantages of LCS include the nice visualization of structure boundaries, revealing the formation of transport barriers. However, the shape of the obtained structures heavily depends on the time window parameter and seeding resolution. LCS-based methods also do not provide a multi-scale representation for coherent structures.

The last set of techniques, called Eulerian or region-based methods, rely on some physical attributes, such as pressure [20], vorticity, Helicity, Q-criterion, Okubo-Weiss criterion and λ_2 criterion [14] and other derived attributes from velocity field. Structure identification is dependent on thresholding. For example, to detect vortices fluid mechanic researchers can play with Q criterion [7] or λ_2 [18] to identify the volume of vortex-like behavior. Many fluid mechanics focus on Eulerian-based approaches because they provide more physical information. It is important to note that the most commonly used physical attributes including Q, vorticity or λ_2 naturally focus on small-scale structures due to its definition, i.e., it is based on vorticity and strain which are inherently small-scale quantities. One way to characterize large (or coarse) -scale structures is to use a convolution kernel - usually an averaging box filter as proposed by Treib et al. [53]. Besides Eulerian methods, moving ensemble averages [32], two-point correlations [48] or Fourier analysis [31] have also been widely used in fluid dynamics. However, they suffer the same issue. Choosing a proper threshold requires a substantial amount of time on trial-and-error experiments which might lead to undesired structures. In this work, we present a parameter-free method to separate large-scale structures.

Vector field decomposition. DMD belongs to the velocity field decomposition methods. In these techniques, the vector field is decomposed into different components as the pre-processing step with hope that the components would help to reveal some desired features. The most well-known method - Helmholtz-Hodge-decomposition (HHD) [3] - decomposes the flow into curl-free and divergence-free vector fields. However, HHD is not applicable for multi-scale coherent structure analysis. Another decomposition method which is considered the most related to DMD is proper orthogonal decomposition (POD) [22] or principal component analysis in statistics. In POD, the data is decomposed into an orthogonal basis of spatial correlated modes, called POD-modes. POD has been commonly applied in fluid mechanics to determine coherent structures from multiple flow snapshots as well as to extract high energy flow features [37], [38], [54] and to improve the vortex detection result [6]. In this work, we propose to use mrDMD to extract large-scale coherent structures from shear turbulent flows. This is the first time the large-scale coherent structures in shear flows are associated with the slowest DMD mode. Also, as shown in Section 6, our mrDMD results characterize physically correct temporal behavior of large-scale coherent structures in shear flows, while the POD results cannot.

3 Background

In this section, we provide the background about shear flows and DMD that our paper is focused on.

3.1 Shear Flows

Shear flows are fluid flows which are driven by a velocity difference. In this work, we are interested in two types of wall-bounded shear flows, i.e., plane Couette flows (PCF) and Waleffe flows. In the following, we provide a brief introduction of these flows and their large-scale structures that domain experts are interested in.

Plane Couette flows (PCF). In simple setting, plane Couette can be described as the flow between two parallel plates separated by a distance d, moving with equal, but opposite velocities $\pm U/2$. A solid body rotation Ω can be added in the spanwise direction that is either anti-cyclonic or cyclonic, i.e., opposite to or in the direction of the shear. The two non-dimensional parameters that define the flow are the (shear) Reynolds number $Re = Ud/\nu$, where ν is the kinematic viscosity of the fluid, and the rotation number $R_\Omega = 2d\Omega/U$. A schematic of the flow is shown in Figure 1.

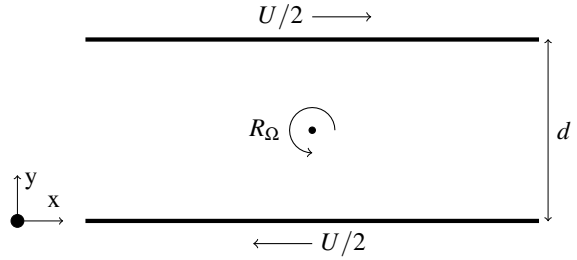

Fig. 1: Schematic of the simulation domain of Couette flow. The streamwise is the x component, while the wall-normal is the y component of the 3D velocity vector. The third (spanwise) dimension z is omitted for clarity.

Depending on the solid-body spanwise rotation, large-scale structures can appear in PC flow. For some values of R_Ω, statistical approaches [39] indicate that they can be pinned in space and regularized in the streamwise direction. As the flow becomes turbulent, structures of increasingly smaller of length- and time-scales appear, even while the large-scale vortices are relatively stationary in time. Detecting the large-scale structures in various parameter settings still remains an open problem that we try to address with our DMD framework.

Waleffe flows. Waleffe flow [9] can be thought of as a variation on plane Couette flow which substitutes the no-slip condition at both walls by a free-slip condition. The system then consists of two parallel plates d apart. The flow is forced by a sinusoidal body shear $F = \cos(\pi y/d)$, which gives a characteristic velocity $U = \sqrt{F/d}$. Waleffe flow has been used to study the effect of the near-wall cycle on the formation and pinning of large-scale structures in shear flow in the absence of a no-slip boundary condition. Pinned and streamwise invariant large-scale vortices were found in the anti-cyclonic regime at high Reynolds numbers [9]. These structures had a different vorticity distribution from those found for the analogous parameters in plane Couette flow, but showed similar temporal behavior when analyzing the separate energy components.

3.2 Dynamic Mode Decomposition

Dynamic mode decomposition (DMD) is a method that provides a spatio-temporal decomposition of data into a set of relevant dynamical modes from a sequence of snapshots of an evolving system [46]. It is capable of *extracting flow structures which evolve linearly*. This characteristic makes it a promising candidate to extract the large-scale structures in wall-bounded turbulent flow, as it is known that these structures behave in a quasi-inviscid, quasi-linear manner [27], [52]. In this section, we first introduce the general idea of the standard (or exact) DMD method, then describe the improved variant – multiresolution DMD (mrDMD).

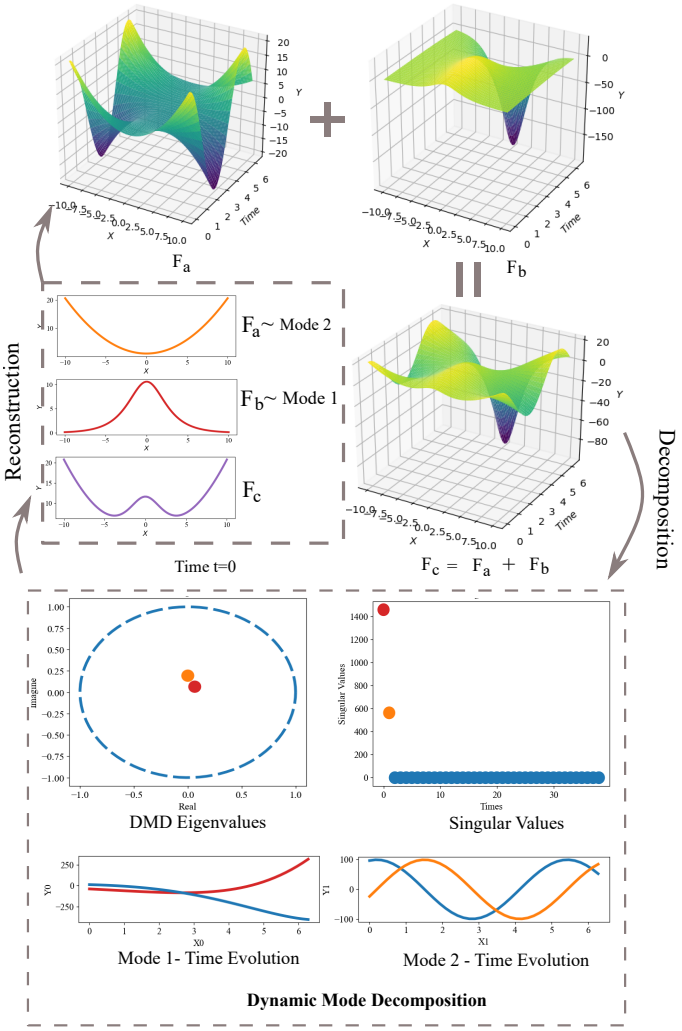

Fig. 2: A sample DMD decomposition process. Given the 2D input function F_c which is the summation of two artificial time-dependent functions F_a and F_b. The DMD extracts the singular values, eigenvalues and a set of modes. The singular values reveal two high-energy modes. Each mode is a complex number and has a time dynamic behavior which is characterized by the position of eigenvalues with respect to a unit circle. In this example, DMD can decompose F_c back to F_a and F_b with the original time dynamics. The red and orange plots in the last row present the real values, while the blue plots demonstrate the imagine parts of the two modes. The X-dimension in the plots presents the time, while the Y-dimension shows the frequency values of the mode over time.

Given an unsteady vector field with M time steps $\mathbf{x}_1 \ldots \mathbf{x}_M$ where $\mathbf{x}_i \in C^N$ is a vector including the velocity field sampled at equal time intervals Δt. In other words, we can generate $\mathbf{x}_i$ by transforming the 2D or 3D flow domain into 1D vector structure in which N is the multiplication between the number of velocity components (i.e., 2 for 2D, 3 for 3D flows) and the domain resolution. Typically, the size of flow domain is substantially greater than the number of time steps, $N >> M$. We can arrange

the data into two column-wise matrices X_1 and X_2 as follows:

$$X_1 = \begin{bmatrix} | & | & & | \\ \mathbf{x}_1 & \mathbf{x}_2 & \dots & \mathbf{x}_{M-1} \\ | & | & & | \end{bmatrix}, X_2 = \begin{bmatrix} | & | & & | \\ \mathbf{x}_2 & \mathbf{x}_3 & \dots & \mathbf{x}_M \\ | & | & & | \end{bmatrix} \quad (1)$$

DMD tries to find the dominant eigenvalues and eigenvectors of a best linear approximation that sends the data from its current state to the next state. The best-fit approximation can be simply expressed as:

$$\mathbf{x}_{i+1} = A\mathbf{x}_i \quad (2)$$

or can be written in the matrix form and decomposed by using Singular Value Decomposition (SVD) as follows:

$$X_2 = AX_1 \text{ or } A = X_2X_1^{\dagger} = X_2V\Sigma^{-1}U^* \quad (3)$$

where A is a $N \times N$ matrix and $\dagger$ denotes the Moore-Penrose pseudo inverse. In practice, N is typically too large; hence, it is nearly impossible to store and compute matrix A directly. Fortunately, DMD circumvents this challenge by analyzing a smaller matrix $\tilde{A}$ obtained via projection onto the left singular vectors in U:

$$\tilde{A} = U^*AU = U^*X_2V\Sigma^{-1} \quad (4)$$

The matrix $\tilde{A}$ is of the size $N \times (M-1)$ which is substantially smaller than the original matrix A, but they have the same eigenvalues as proven by Tu et al. [16]. After applying the eigen-decomposition to $\tilde{A}$, we can arrange the eigenvalues λ_i and eigenvectors w_i in the matrices Λ and W such that:

$$\tilde{A}W = W\Lambda \quad (5)$$

The eigen-decomposition of A can be defined as:

$$A\Phi = \Phi\Lambda, \text{ where } \Phi = X_2V\Sigma^{-1}W \quad (6)$$

The columns of Φ are called DMD modes. They have the same size and spatial configuration as $\mathbf{x}_i$, except that each mode has a specific temporal behavior characterized by the corresponding eigenvalue λ in Λ. We can derive the DMD representation of a data snapshot based on the columns of matrices A and Φ:

$$x_{DMD}(t) = \sum_{k=1}^{K} \phi_k e^{(\delta_k + iw_k)t} a_k \quad (7)$$

where $\delta_k + iw_k = \frac{\log(\lambda_k)}{\Delta t}$. δ_k is the growth rates, and w_k is the frequency of the DMD modes ϕ_k which behave similarly as Fourier. The amplitudes a_k can be derived from the least squares fitting of the snapshots during the expansion. $K \leq M$ is the number of modes. $\mathbf{x}_{DMD}$ is real if $K = M$; otherwise (i.e., $K < M$), it can be complex. To obtain a reconstructed field with real values, the linear combination of the real and imaginary parts of $\mathbf{x}_{DMD}$ can be used, as they are both solutions to Eq.(2) [24]. The entire process of DMD computation reveals several important components and characteristics of the method. Given a 2D random time-dependent sample data as illustrated in Figure 2, we can visualize the singular values of X_1 which show the low and high-energy modes. The number of high-energy modes can be used to reduce the dimensionality of the system and be utilized for the data compression task. Instead of storing the full spatial-temporal flow field, we just need to retain the prominent modes and their corresponding eigenvalues for data reconstruction. Readers who are interested in how to choose the suitable number of modes are referred to the work by Jovanović et al. [21]. The visualization of DMD modes and their eigenvalues are shown in Figure 2. The dynamic behavior of a DMD mode depends on the values of its corresponding eigenvalue with respect to a unit circle. The mode either grows, decays, or neither if the eigenvalue is outside, inside or seats exactly on the unit circle. There is an oscillation if the eigenvalue has a *non-zero imaginary part*. The time dynamic evolution of the sample DMD modes are computed and visualized in the last row of Figure 2. *DMD modes also can be characterized by the speed of the time evolution*. For instance, the second mode has a higher frequency (as indicated by their quick changes) which makes it the fast modes, while the first mode is a slow mode as it moves/changes relatively slower.

Many methods have been proposed to address the question about the best mode selection. For example, Gavish et al. [12] have found out the optimal cutoff value for truncating singular values so that only important modes with less noise data remain. Sparsity-promoting DMD [28] is another approach which tries to find the minimum number of modes to reconstruct data. Our goal is to find the modes that can capture both spatial and temporal behavior of the large-scale coherent structures. The large structures tend to stay longer than the small-scale ones; hence, longevity is one of the main selection criteria.

Relation between slow DMD modes and large-scale coherent structures. As shown in previous works [33], [57], DMD modes can be used to extract spatial configuration and temporal information of certain coherent structures. Some works [58] argue that the DMD modes and their corresponding temporal evolution plots can separate coherent structures in spatial and spectral sense (according to their temporal behavior – grows, decays, or oscillates). Although this is not rigorously justified and not all flows have the exact same number of structures as the number of DMD modes, there is an important observation that motivates us to use certain DMD mode(s) to identify large-scale structures in the shear flow. That is, both the slow mode and the large-scale structures change/move slowly over time. For large-scale structures, this is because they have a larger inertia due to their higher kinetic energy. This observation leads us to develop an effective framework to separate large-scale structures from small ones in shear flows using DMD (Section 5). Note that, this relation between slow DMD modes and large-scale structures need not be true for other flows than shear flows (e.g., translational flows), which we will discuss in Section 7.

It has been shown that the standard/exact DMD cannot sufficiently handle the transient time phenomena (e.g., features exist for a short period of time) that often occur in the beginning of many turbulence flows (including shear flows) before a stable state is reached [24]. To address this issue and develop a robust and generalized DMD-based analysis and visualization framework for different flows, we resort to a variant of DMD, called multi-resolution DMD (mrDMD).

3.2.1 Multi-Resolution DMD

Motivated by foreground/background subtraction in video processing, mrDMD tries to separate the slow and fast modes. As we mentioned in the previous section, the slow mode has a relatively low frequency or slow growth/decay rate. They can be defined by small values of both the growth rates δ_k and frequency w_k. To obtain the slow modes, we can plot them in a complex unit circle $(Re(\log(\lambda_k)), Im(\log(\lambda_k)))$. The nearer to the origin, the slower the corresponding DMD modes are.

mrDMD is a recursive process in which the slow modes are removed iteratively, and the remaining data is filtered for

analysis of its higher frequency content. The entire process can be described below:

1) Compute DMD for the existing data.
2) Determine fast and slow modes relatively based on the values of w_k and δ_k.
3) Reconstruct data with only slow modes
4) Subtract the reconstructed data by the slow modes from the available data
5) Split the remainder data in half in time
6) Repeat the procedure for the first and second half of the remainder data separately (including this step)

Note that standard DMD can be considered as a special case of mrDMD when only one level mrDMD is performed with the additional benefit of the identification of the slow modes, which is needed for our problem.

4 Parallel Implementation for mrDMD

Due to the high memory consumption of the DMD computation, previous works on DMD focus on 2D or small 3D flow data. Recently, many efforts [35], [45] have been made to improve the computation of DMD. Pendergrass et al. [35] proposed a parallelized algorithm to compute the dynamic mode decomposition (DMD) on a graphics processing unit using the streaming method of snapshots singular value decomposition. Sayadi et al. [45] employed the parallel Tall-Skinny QR(TSQR) algorithm to the DMD, allowing the decomposition of very large datasets. To our best knowledge, there is no existing parallelized implementation for mrDMD, which we address next.

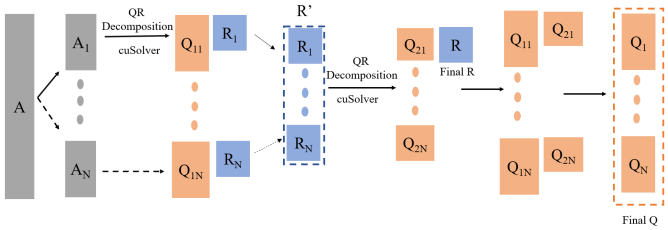

Fig. 3: The pipeline of the direct TSQR algorithm in which the tall-and-skinny input matrix A is decomposed into smaller pieces so that they can fit into the GPU memory. QR decomposition is performed on each subset of the matrix A, then the outputs are combined in order.

The fundamental computation of DMD is based on SVD. We can compute SVD of a matrix A through the QR decomposition as follows:

$$A = U\Sigma V^* = QR = QU_R\Sigma_R V_R^*, \text{where } [U_R, \Sigma_R, V_R^*] = svd(R) \quad (8)$$

The left singular vectors U_i of A are computed by using $U_i = Q_i U_R$. The singular values and the right singular vectors are already stored in Σ_R and V_R^*, respectively. The parallel pipeline of QR is illustrated in 3. The input matrix A is decomposed into sub-sets which have the same number of columns, but smaller number of rows. Traditional QR decomposition is performed on each subset in a single processor core.

Once we construct the DMD computation based on the parallelized SVD, mrDMD is implemented based on the algorithm described in Section 3.2.1 [1]. We utilize the open-source cuSOLVER [30] to perform the Eigenvalue and QR decomposition,

1. The source code of a reference implementation of mrDMD will be made available upon the acceptance of this work.

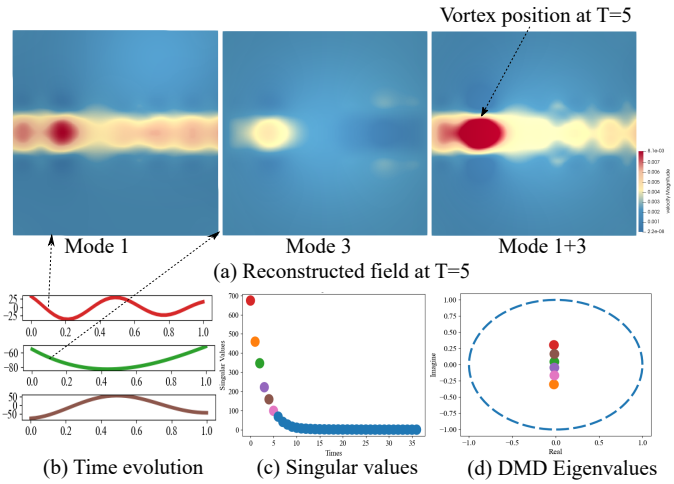

(a) Reconstructed field at T=5
(b) Time evolution (c) Singular values (d) DMD Eigenvalues

Fig. 4: Sample reconstructed field using DMD modes and their time evolution from the Tube simulation. (a) The two DMD reconstructed fields shows different intensity of the main vortex at time $T = 5$. Combining two modes reveals a correct position of the main vortex at the selected time. The last row presents the plots of (b) the time evolution, (c) singular values, (d) DMD eigenvalues and of DMD modes.

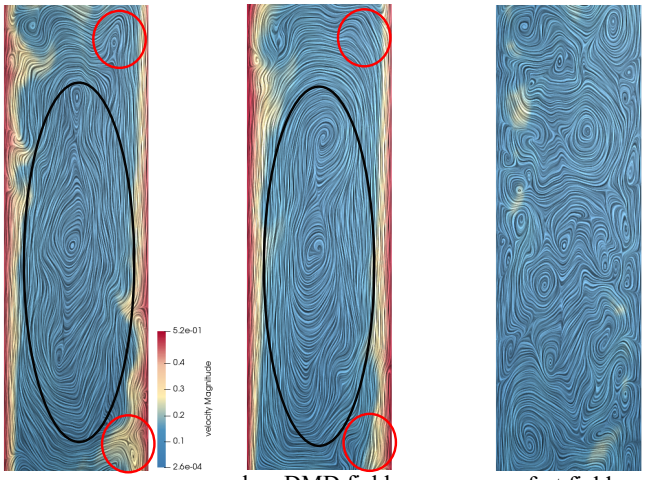

original field − slow DMD field (a.k.a large-scale CS) = fast field (a.k.a small-scale CS)

Fig. 5: The relation between the original and reconstructed DMD fields in the plane Couette flow with $R_\Omega = 0.1$. The 2D Taylor vortices depicted by black circles are the target large-scale CS in the simulation. The large structures can be observed clearly in the DMD reconstructed field. Small-scale features near the wall are highlighted in the red circles in the original field. The small features are revealed in the subtracted field.

as well as cuBLAS for the large matrix multiplication. The performance evaluation of our GPU implementation of mrDMD can be found in the supplemental document.

5 Large-scale Structure Separation using mrDMD

In this section, we discuss the properties of DMD modes and their eigenvalues which make them suitable for the large-scale coherent structure extraction problem. A coherent structure is characterized by temporal and spatial information. We can use DMD eigenvalues to characterize the temporal persistence of structures. Basically, DMD is a Fourier-based decomposition process. Each DMD mode

has time dynamics defined by a single complex eigenvalue. We can reconstruct the original field by taking the summation of all mode values. However, the contribution of each mode at any given time is different, as controlled by the frequency of the eigenmodes. The frequency also indicates the movement speed of the mode: at larger frequencies the DMD mode changes faster. Similar to matrix eigenvectors, each mode is normally normalized to have a unit norm/magnitude.

For the spatial extraction of coherent structures, we can rely on DMD modes as they capture all of the spatial features existing in the flow domain. *If structures evolve linearly, then they will coincide with the DMD modes*. For example, Figure 4 shows two DMD modes generated with a simple Tube simulation. In this simulation, a vortex tube starts from the left side of the domain and moves to the right side, then breaks down. We take a cross section of the original 3D simulation [2] in this example. It can be seen from the two DMD modes that both of them can capture some positions of the main vortex over time. However, the magnitudes of the vortex in each mode are varied. Indeed, a DMD mode works as a projection plane where we can take all the spatial features and project them on the plane, but with different intensity. To reconstruct the features in the original data, we simply add the weighted modes with the weights determined by their temporal magnitude as shown in the bottom plots of Figure 4 and Eq.(7). Note that this reconstruction takes into account both the real and the imaginary parts of the modes and their time evolution characteristics, while in all visualizations of modes only real parts of the modes are shown.

The next step is to determine the modes that have our desired features. As the large-scale structures move slowly as discussed in Section 3.2.1, the corresponding indicators - slow DMD modes (especially the slowest mode) - become an ideal candidate to characterize these large-scale structures. With our fast mrDMD, we can identify the slowest mode from each iteration (or level) of DMD, and use it and its time evolution to reconstruct a flow as the input for large-scale structure visualization. In our experiments, we found the slowest mode from the first level of mrDMD most effectively captures the large-scale structures in shear flows (Section 6). Once the large-scale structures are separated in the flow reconstructed from the slowest DMD mode, the small-scale structures can be studied in the flow by subtracting the DMD reconstructed flow from the original flow, as shown in Figure 5. The study of the small-scale structures in shear flow is beyond the scope of this work, which we will leave for the future work.

We wish to point out that when utilizing DMD for flow analysis and interpretation, visualizing the reconstructed flow from the selected modes often provides more intuition of the spatio-temporal behaviors of the flow than only visualizing modes and their time evolution that may miss some information (i.e., the imaginary part of the modes and time evolution).

6 Applications

We have applied our mrDMD based large-scale structure separation framework to the two main types of shear flows, namely the Couette and Waleffe flows. Their configuration is described in Section 3. We look at several 3D Plane Couette simulations that are generated with different anti-cyclonic solid-body rotation ratios R_Ω ranging from 0 to 0.1. Waleffe flow is simulated with a Reynolds number $Re = 3.16 \times 10^3$ and an anti-cyclonic rotation ratio R_Ω =0.63. For these control parameters, Farooq et al. [9] recently used the autocorrelation and other statistic-based methods to prove that large structures exist in the Waleffe flow. We demonstrate that the slow DMD modes can reveal similar well-known large-scale features in both Plane Couette and Waleffe flows. By using the obtained slow DMD modes, we can isolate the large structures without threshold selection.

TABLE 1: Performance of DMD on three datasets

Dataset	Spatial Resolution	Time Steps	Running Time (minutes)
2D plane Couette	1024×512	100	6.45
3D plane Couette	$512 \times 384 \times 256$	40	32.6
3D Waleffe	$512 \times 384 \times 256$	80	124.38

(a) FTLE values from the original vector field

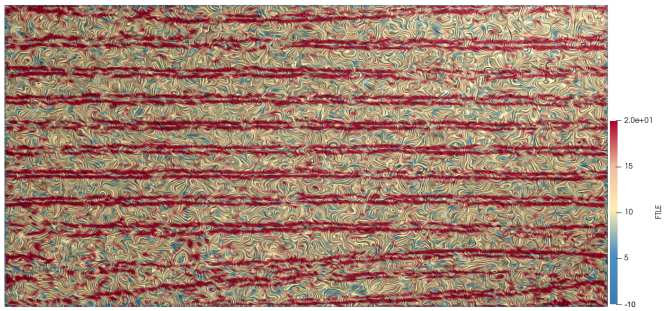

(b) FTLE values from the DMD reconstructed vector field

Fig. 6: The FTLE values computed from (a) the original vector field and (b) the reconstructed field with the slowest DMD mode on a Plane Couette flow with $R_\Omega = 0.1$. The cut is at the centerline of the wall-normal. The first time step is shown. The LCS structures in (a) do not reveal any meaningful patterns, while in (b), the structures clearly show horizontal ridges which are the boundaries between two counter-rotating Taylor vortices.

For each Couette and Waleffe flow, we generate a set of 2D and 3D snapshots. We use 2D datasets to verify and compare our results to the existing works of Taylor Couette and Waleffe flows that are mainly focused on their 2D counterparts. One of the main reasons that looking at 2D cross section of these flows may be sufficient is that the large structures exist along the streamwise direction; thus, fluid mechanic researchers can perform analysis on 2D streamwise-spanwise planes. We also use 2D data to evaluate the effect of time windows on the final DMD modes.

The fast GPU implementation can enable us to process the 3D snapshots of Taylor Couette and Waleffe flows for the first time. However, a large time window is still a challenge for the 3D analysis because the memory required to store the 3D data is beyond the physical memory of our workstation. An out-of-core, streaming implementation of mrDMD is needed, which is beyond the scope of this work. The timing information of our mrDMD when applied to the shear flows used here is provided in Table 1.

2D-slices of a plane Couette flow- R_Ω=0.1. In the first experiment, we apply mrDMD to 2D slices of a Plane Couette simulation

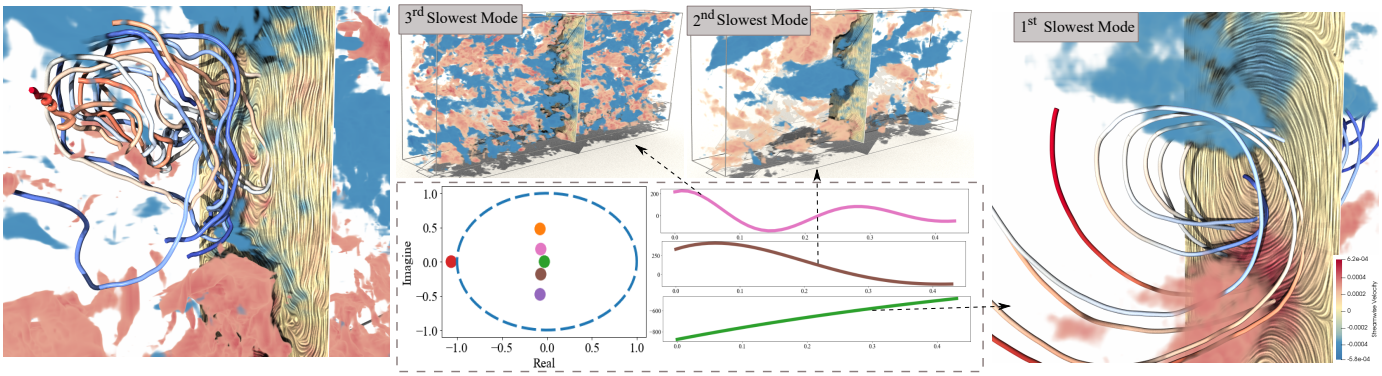

(a) Turbulent Shear Flow (b) Multi-resolution Dynamic Mode Decomposition (c) Large-scale Coherent Structures

Fig. 7: We apply the multi-resolution Dynamic Mode Decomposition (mrDMD) to extract large-scale coherent structure for turbulent shear flows. (a) shows a closeup view of the input Waleffe flow. The colors are mapped to the streamwise velocity, i.e., the x component of the velocity vector with red means positive blue for negative. (b) demonstrates a few DMD modes that correspond to coherent structures of different scales for this flow. Each mode is sufficiently characterized by their eigenvalues shown in the unit circle plot and their respective time evolution plots. (c) the slowest DMD mode characterized by the slowest change in its time evolution plot is used to represent the large-scale structure of this flow that also has a slow dynamic. The three modes of the entire flow domain can be found in the supplemental document.

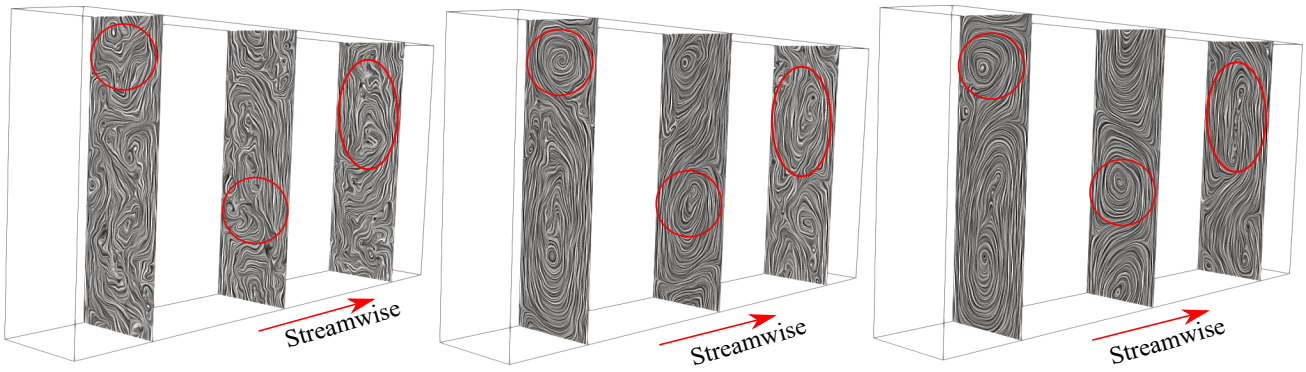

(a) Original field (b) DMD Mode (c) Time-Average

Fig. 8: Results of a 3D Waleffe flow with $R_\Omega = 0.63$. The first time step is shown. Three slice cuts along the streamwise direction at $x = 1$, 3.14, and 5 are shown, respectively. (a) The original field is very turbulent. It is impossible to visually distinguish the large-scale feature. (b) The large-scale coherent vortices appear clearly in the DMD mode. The extracted vortices behave similarly to Taylor vortices. This observation is verified by the result of the recent work [9]. (c) Time average velocity field also reveals similar structures, but their temporal information is discarded.

with $R_\Omega = 0.1$. The 2D data is obtained by taking the slice planes parallel to the walls (i.e., along the streamwise direction) at the mid-gap. It is important to mention that the Taylor vortices - the prominent large-scale structures - are fully formed with $R_\Omega = 0.1$. Thus, this simulation is an ideal candidate to verify the correctness of the selected DMD modes. Three hundred time steps are collected and input to our mrDMD program. It is known that Taylor vortices of this flow are counter rotating. Instead of extracting the individual vortices, we extract the transportation barriers that separate them by computing the FTLE fields. Figure 6 shows the comparison between the FTLE values computed from the original vector field and those from the reconstructed vector field using the slowest DMD mode, respectively. The LCS structures in Figure 6(a) do not reveal any meaningful patterns, while in (b), the structures clearly show horizontal ridges which are the boundaries between two counter-rotating Taylor vortices. This example shows that our DMD-based method can help better capture the large-scale structures that separate the Taylor vortices.

3D Plane-Couette - R_Ω=0.1. We apply our mrDMD based method to full 3D snapshots of a Plane-Couette simulation with a smaller boundary size than the 2D version. Again, the Taylor vortices are the large-scale structures in this simulation setting. The resolution for the 3D spatial domain $NX \times NY \times NZ \times NT$ is $512 \times 384 \times 256 \times 40$. The total data size is 36GB. It took our framework 32.6 minutes to process this data. As shown in Figures 5, the large-scale structures - Taylor vortices (indicated by black circles) - are hardly observed in the original field, while they can be revealed clearly in the extracted slow DMD mode. Small-scale features near the wall are highlighted in the red circles in the original field. These small features are considered as noise, and they make the separation of the large structure challenging. Our DMD-based method can filter out these small-scale structures. As shown in Figure 12(a), the slowest DMD mode of this field more effectively reveals the large-scale separation structure that separates the individual Taylor rolls/vortices. Note

(a) Streamlines

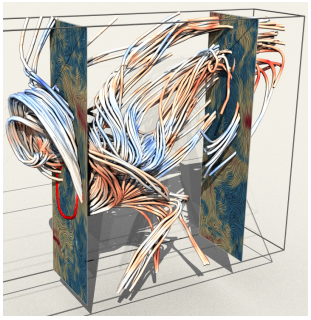

(b) Pathlines in the original field

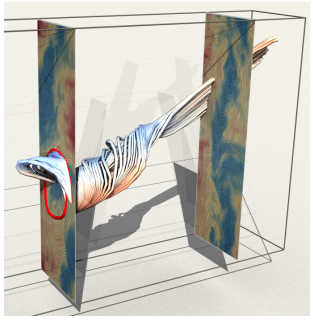

(c) Pathlines in the DMD reconstructed field

Fig. 9: Results on the 3D Waleffe flow with $R_\Omega = 0.63$. (a) The iso-surfaces of the velocity streamwise component in the slowest DMD mode. The roll-like structures separate two neighboring large-scale structures. The streamlines depict the shapes of the large structures along the streamwise direction. (b)(c) Pathlines in the original and the DMD reconstructed field are generated with the same seeding curve (the red line). The pathlines in DMD reveal a vortex-alike structure similar to (a) due to the almost stationary characteristic of the structure.

that the separation layers or the iso-surfaces in 3D correspond to the iso-contours in the 2D results (please refer to the supplemental document for more details).

3D Waleffe - R_Ω=0.63. The Waleffe flow is simulated with the Reynolds number $Re = 3.16 \times 10^3$ and the rotation ration $R_\Omega = 0.63$. A recent work [9] has demonstrated that the large-scale structure emerges with this optimum rotation ratio. We collect 80 continuous snapshots with a spatial resolution of $512 \times 384 \times 256$. The three slowest DMD modes are shown in Figure 7 and the supplemental document. Again, we select the slowest mode which is nearest to the origin of the unit circle. The second, third, fourth and fifth modes are provided as the references to compare with the slowest mode. The faster the modes, the more small-scale features they can reveal. It is interesting to point out that their eigenvalues have the identical real parts, but they have different imaginary parts. As the result, their corresponding time evolution plots are similar. Figure 8 shows the difference between the original field and the extracted slow mode. The original field is turbulent, including many small-scale features. It is difficult to observe any prominent large-scale features. In contrast, the extracted slow DMD mode helps to reveal the structures similar to the Taylor vortices seen in the above 3D Taylor Couette flow. In the most recent work [9], these structures are reported as the large-scale coherent structures for the Waleffe flow. We use the 2D slice cuts at different positions along the streamwise direction to highlight the shape of the prominent structures.

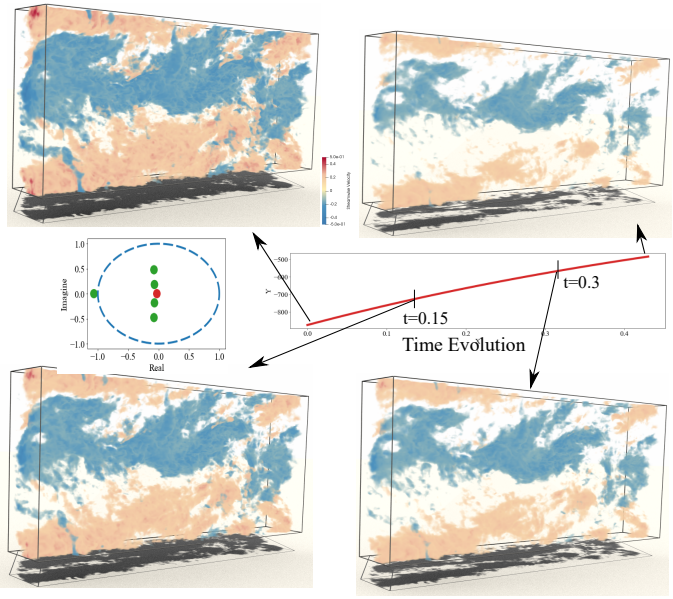

Fig. 10: The volume rendering of the streamwise velocity of the reconstructed field using the slowest DMD mode at a number of sampled times. Although the time evolution is increasing, their values are negative; thus, the structures become weaker.

After the filtering process, we can extract iso-surfaces based on the streamwise velocity component of the DMD mode as shown in Figure 9. These iso-surfaces form a layer to separate two neighboring large-scale structures, which is similar to 3D Taylor Couette flow, as indicated by the seeding streamlines that are circulating around some common curves. However, the large-scale structures revealed in the Waleffe flow are not always invariant along the streamwise direction in contrast to the Taylor rolls seen in the Taylor-Couette flow. This result solidifies the intuition already hinted by the data and visualizations in [9]: the Waleffe flow large-scale structures are not exactly analogous to those of Plane Couette flow but present some oscillations in the spanwise direction. This state-of-the-art fully three-dimensional visualization will be useful to precisely characterize the difference between the large-scale structures in Waleffe and plane Couette flow in the future.

6.1 Comparison with other approaches

Comparison with POD. We apply POD to the Waleffe flow and extract the first ranked mode or the most energetic mode. The results are shown in Figure 11. In terms of the geometric or spatial representation, POD can capture the similar patterns as DMD. However, from the physical point of view, the coherent structures are not defined just by shape and position, but also by the temporal behavior like how fast or slow they are moving overtime. It is also worth highlighting that the POD modes do not change with the input snapshots that are reordered, which means the modes do not depend on the time evolution or dynamics existed in the data [16]. As demonstrated in Figure 11(a), the reconstructed flow field from POD is not temporally coherent (i.e., its kinetic energy changes arbitrarily over time), which is not physically plausible. In contrast, the flow reconstructed from the slowest DMD mode and its corresponding time evolution has smooth transition of its pattern and kinetic energy, which is more physically meaningful and accurate. POD and DMD use different criteria to compute

the modes. The POD seeks for the optimal approximation via a principal component analysis (PCA), while the DMD tries to obtain the best linear dynamical system describing the input data. POD is a statistical decomposition technique that does not tell us much more about the modes that it finds, and further processing must be done on them. This is unlike the information which can be obtained from a DMD decomposition: time evolution of the spatial features, where we know the modes evolve linearly and with a certain dynamics given by the characteristic frequencies. The fact that the structures revealed from the slowest DMD mode match the expected large-scale structures in shear flows (Figure 13) in part supports a recent intuition in the fluid mechanism, that is, the large-scale structures in shear flows behave in a quasi-linear manner [27], [52]. The advantages of DMD over POD have also been reported in many other published works in fluid dynamics. [16], [24], [25].

Comparison with the simple time average of the original flow. It is shown that a simple time average (e.g., average all velocity values at the individual spatial locations over time) may reveal the existence of certain structure with slow change over time in the flow. In particular, large-scale structures that move slowly would be emphasized in the average flow due to their continuous contribution to the average computation, as shown in Figure 8 (c). Nonetheless, the average flow loses the temporal information of the flow features. In contrast, even though the slow DMD mode is similar to a single snapshot of the flow, it is accompanied by the information of its contribution to the flow over time (characterized by the time evolution plot); thus, it naturally encodes more temporal information of the flow than a simple time average. In the example shown in Figure 8, both the time average (c) and the slowest DMD mode (d) reveal similar large-scale structure of the 3D Waleffe flow. However, by multiplying the time evolution plot, the DMD mode reveals certain temporal behavior of the extracted structure, while the time average cannot.

Comparison with convolution kernel based method [53]. Another popular approach for revealing large-scale structure is to perform a convolution kernel based filtering. We compare our DMD-based method with the convolution kernel based filtering in Figure 12. In particular, the extracted large-scale structure using our method is shown in Figure 12 (a), while the result of the convolution kernel based is in (b). From the comparison, we see that the convolution kernel-based method can also reveal the positions of the large structures, but it is threshold dependent and may significantly alter the velocity field as shown in (b). In contrast, the slow DMD mode gives the most meaningful result which retains the main features from the original field, while the small vortices near the walls are removed. More importantly, our DMD-based method does not require any thresholding trials.

To further verify which field better captures the large-scale structure in the 3D Plane Couette flow, we compare them with the approximate boundary surfaces of the large-scale structures extracted using Nguyen et al.'s approach [29] (Figure 12(c)). From this comparison, we see the streamlines obtained in the DMD reconstructed field better assemble the structures as indicated by the boundary surfaces than those obtained in the smoothed field using the convolution kernel smoothing. In the future, it will be important to develop a robust technique to extract the large-scale structure from the DMD reconstructed field.

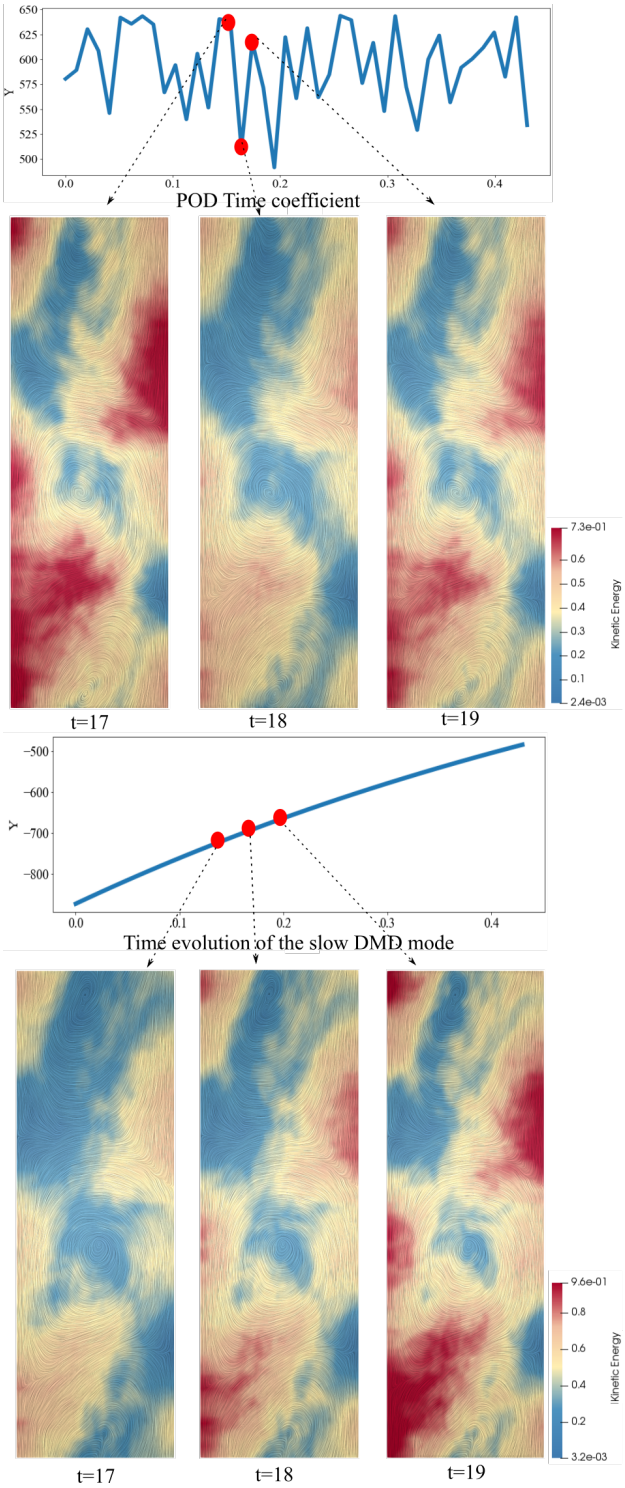

Fig. 11: Comparison between POD and DMD on the Waleffe flow. The cuts are at the center of the streamwise direction for the Waleffe flow. Although the spatial representation of large-scale structures are observable in both the slowest DMD mode and the first POD mode, POD cannot characterize the temporal characteristic of the structures. In the three consecutive time steps selected (red dots), the kinetic energy varies significantly in POD contradicting to the slow change expected for the large-scale structures. In contrast, the slow motion of the structure is captured accurately by the DMD method as shown by its smooth time evolution plot.

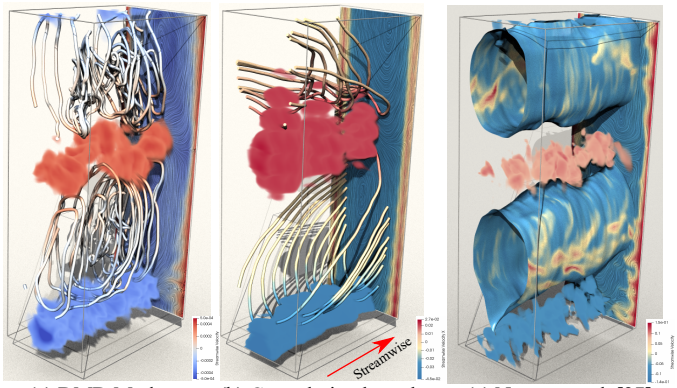

(a) DMD Mode (b) Convolution kernel (c) Nguyen et al. [27]

Fig. 12: Comparison between DMD, the convolution kernel and Nguyen et al. [29] approaches on the 3D Plane Couette flow with $R_\Omega = 0.1$. Volume rendering show the prominent structures in the DMD mode (a), and the smoothed field using a convolution kernel (b). Streamlines in (a) capture the expected Taylor roll structures better than the ones in (b) as the top structure is distorted due to the over smoothing. (c) The approximated surfaces by Nguyen et al.'s method reveal the similar large-scale structures as shown by streamlines in (a)

6.2 Other Modes Returned by mrDMD on Shear flows

Slow modes in higher-level mrDMD. mrDMD is an iterative algorithm that can provide multiple levels of slow modes and their corresponding temporal evolution. After the first level, the lowest-frequency or slowest modes are removed from the data. The remaining data having more dynamic behavior is used for the next level. It means that the slow modes in the second level are faster than the ones in the first level. Since the large-scale structures of interest are mostly stationary or move very slowly in shear flows, the slowest mode in the first level is sufficient. This observation is demonstrated in Figure 13(a) which shows three slow modes in the first levels, and the slowest modes in the other levels. The large-scale structures are only observable in the first level. The higher level modes are useful for capturing transient phenomena, handling the translational and rotational invariant in the data [24]. These properties do not exist in the large-scale coherent structures of shear flows. In the next section, we discuss the application of mrDMD for non-shear flows in which the higher level modes can be used to extract coherent structures that have translational property. Note that selecting the single slowest mode in the first level is parameter-free. However, choosing the number of levels and a sufficient number of slow modes in each levels is a parameter dependent process. It is still an open problem and beyond the scope of our work.

Other slow modes in the first level mrDMD. Figure 13 (b) shows the other slow modes in the first level mrDMD. Compared to the slowest mode, these slow modes do not encode the expected large-scale structures of this flow.

Complex conjugate DMD modes As described earlier, DMD modes can be complex. If a mode and its corresponding eigenvalue are complex, there must be another complex mode conjugate to it given a real-valued linear system expressed by Eq.(2) [5]. If there are two conjugate slowest DMD modes in a general flow, we use both of these modes and their corresponding eigenvalues

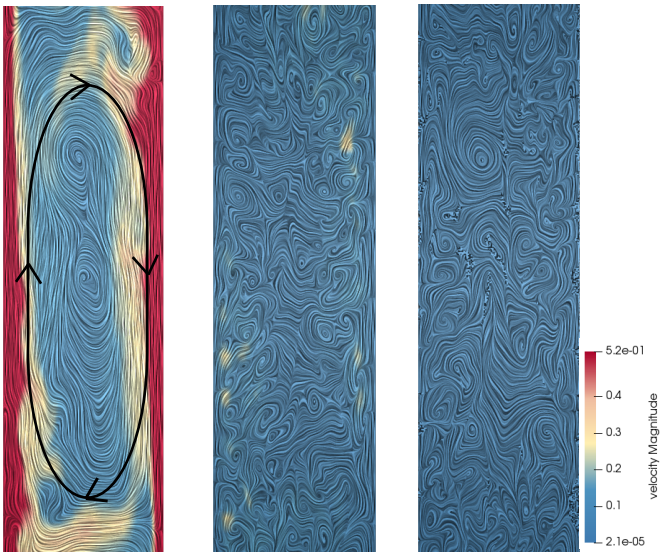

1st level 2nd level 3rd level

(a) The slowest modes in the different MrDMD levels

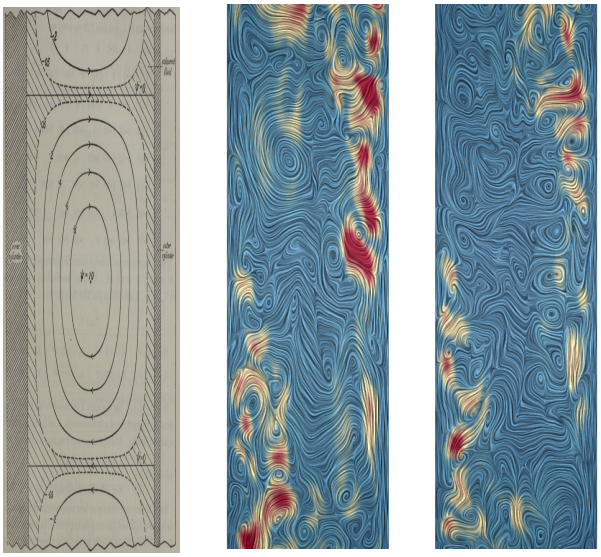

Taylor vortices 2nd slow mode 3nd slow mode

(b) (right) The illustration of Taylor vortices [51] and (left) two modes in the first mrDMD level

Fig. 13: Slow modes in different levels of mrDMD. The large-scale coherent structures are only able to be observed in the slowest mode of the first level. These structures are called Taylor vortices which was first introduced and illustrated by G. I. Taylor [51].

to reconstruct the field, which will lead to a real $\mathbf{x}_{DMD}$. See the supplemental document for a proof. Nonetheless, the slowest DMD modes in the shear flows that we experiment with are purely real, because large-scale structures in shear flows are stable and do not oscillate, leading to vanishing imaginary part of the corresponding eigenvalue [16].

7 mrDMD on Non-Shear Flows

To evaluate the effectiveness of the proposed method for the coherent structure extraction task in non-shear flows, we perform an experiment with a vortex ring simulation which simulates a vortex ring hitting a wall with a Reynolds number of 2000. We take the 2D cross section of this simulation as input [2]. The

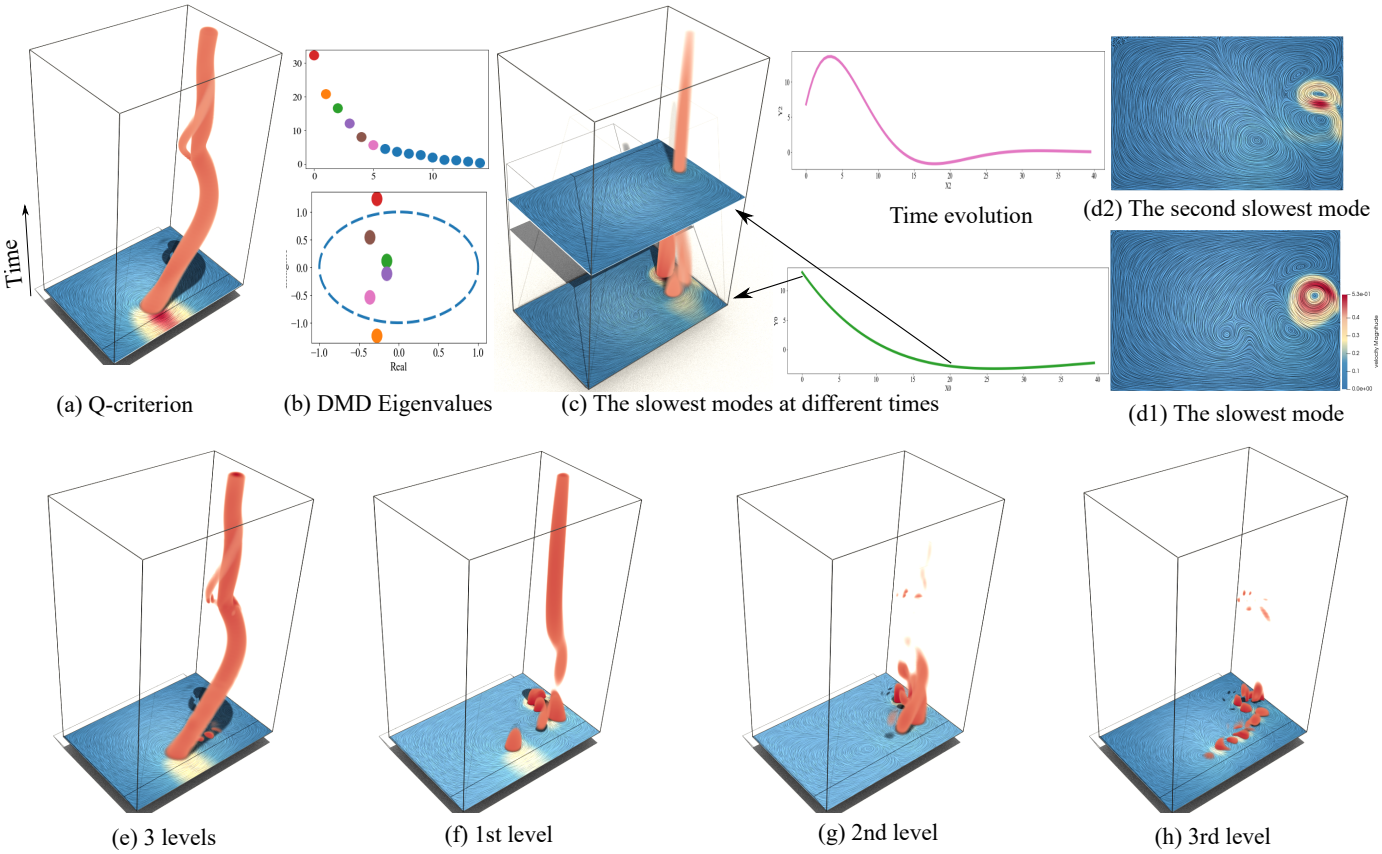

Fig. 14: The mrDMD results of the 2D vortex ring simulation. (a) The volume rendering of the Q-criterion field illustrates the behavior of the original flow where a primary vortex starts near the center of the domain and gradually moves toward and eventually hits the wall, which induces a shear layer at the wall that lifts a secondary vortex. (b) The plot of the singular (top) and DMD eigenvalues(bottom). Note that the ranks of the singular values do not correspond to the position of the DMD eigenvalues in a unit circle. (c) Volume rendering of the Q-criterion derived from the reconstructed field by using the slowest modes. The two time slice cuts show the evolution of the slow mode over time. The slowest mode only captures the behavior of the flow after the primary vortex hits the wall. Two slow modes are shown in (d1)(d2). The volume rendering of Q-criterion derived from the reconstructed field by using (e) slow modes in three levels, (f) three slow modes in the first level, (g) two slow modes in the second level, and (g) one mode in the third level. We need to combine multiple levels to capture the behavior of the main vortex structure.

flow motion is illustrated in Figure 14(a). During the interaction with the wall, the primary vortex (i.e., the cross section of the vortex ring) approaches the wall and induces a boundary shear layer. As the vortex slides against the wall, the boundary layer becomes unstable and is lifted up as a secondary vortex, which in turn lifts up the primary vortex. This data set helps us analyze the role of coherent structures interacting with boundaries, and the generation of turbulence in wall-bounded flows. The flow is a transient flow, and contains several phenomena within, rather than being a purely shear flow. Because of the high-Reynolds number, we do not expect that at any level this flow has structures that behave quasi-linearly. Our mrDMD result is shown in Figure 14 (b–d). There are two pairs of symmetric eigenvalues (b). The two slow modes shown in Figure 14(c1)(c2) are selected from one eigenvalue of each of the two pairs. The reconstructed field using these two modes according to their time evolution plots is shown in (d). As can be seen, the primary vortex before impacting the wall is completely lost in the reconstructed flow. This indicates that while the slow DMD modes provide a mathematically correct decomposition, they do not capture any relevant physical modes in this case. Specifically, they fail to capture the complete behavior of the primary vortex which is the dominant feature in the flow. This simple example shows that DMD (a linear approximation of unsteady flows) may not work well with flows that are not quasi-linear. However, how to determine whether an unsteady flow is quasi-linear or not is not a trivial task, which is beyond the scope of this work yet is important to achieve in order to provide a more accurate guideline for the application of DMD framework.

8 Conclusion

In this paper, we introduced to the visualization community a large-scale coherent structure identification framework for shear flows based on the recently popular dynamic mode decomposition (DMD). Our method is based on an observation between the slowest DMD mode and the large-scale structures seen in the shear flows. In particular, we show that the slow DMD mode characterizes the coherent structure that has a slow temporal evolution, which shares some similarity to the large-scale structures in the shear flows that also change slowly. Based on this observation, we propose to use the slowest DMD mode to help identify the large-scale structures in the shear flows. To address the issue of the standard DMD in handling transient time events, we resort to multi-resolution DMD (mrDMD) to identify the slow mode.

To address the slow computation of mrDMD, we provide a new CUDA implementation. We demonstrated that our DMD based strategy can help better reveal the large-scale structures from a number of 2D and 3D unsteady shear flows than existing methods. Finally, we apply our method to some non-shear flows that do not behave quasi-linearly. Our results show that DMD fails to capture the essential behavior in those flows, which further suggests that *DMD should be applied primarily to quasi-linear flows in order to reveal physically meaningful structures.*

Limitation and future work Although our work shows the promising use of DMD in identifying large-scale structures from shear flows, there are a few limitations that we aim to improve. First, the structure revealed by the DMD modes need not be the structure of interest to the experts. In particular, DMD can be biased to structures that are better characterized by the attributes used for DMD computation (i.e., velocity field in our work). For example, in the 3D Plane Couette flow, while the large-scale structures of interest are the Taylor rolls, our DMD method reveals the separations structures between the individual rolls. This is because the flow inside the Taylor roll has small velocity in comparison with that at the boundary of two rolls. Second, the information encoded by the slowest DMD mode along with its time evolution plot need not fully represent the large-scale structures. This is apparent because the patterns in the reconstructed field using a DMD mode are fixed with only varying amplitude over time. A possible way to address this is to choose a number of slow modes that complement each other over time to represent the large-scale structures. mrDMD also provides a hierarchical mechanism with multiple levels of modes. In this version, we only utilize the slowest mode in the first level which is suitable for the large-scale coherent extraction task. Investigating the sub-modes are also promising to characterize the hierarchical behavior of flow features. To select the adequate modes from different levels, we can adapt recent works (c.f. [23]) on the visualization and analysis of DMD results. Third, even though we implement a fast mrDMD using CUDA, it does not address the memory constraint for large-scale data. In the future, an out-of-core implementation will be needed for it to process the large-scale 3D turbulence flows. Finally, DMD computation is not objective. While this is not an issue for the large-scale structure extraction for shear flows due to their dominance and slow motion, it may still be important to achieve objectivity for other type of flows, which should be investigated in a future work.

ACKNOWLEDGMENTS

We would like to thank the anonymous reviewers for their valuable feedback and comments to this work. This research was supported by NSF IIS 1553329.

REFERENCES

[1] V. Avsarkisov, S. Hoyas, M. Oberlack, and J. García-Galache. Turbulent plane couette flow at moderately high reynolds number. *Journal of Fluid Mechanics*, 751:R1, 2014.

[2] M. Berenjkoub, R. O. Monico, R. S. Laramee, and G. Chen. Visual analysis of spatia-temporal relations of pairwise attributes in unsteady flow. *IEEE transactions on visualization and computer graphics*, 25(1):1246–1256, 2019.

[3] H. Bhatia, G. Norgard, V. Pascucci, and P. Bremer. The helmholtz-hodge decomposition—a survey. *IEEE Transactions on Visualization and Computer Graphics*, 19(8):1386–1404, 2013.

[4] E. Bodenschatz, W. Pesch, and G. Ahlers. Recent developments in rayleigh-bénard convection. *Annual Review of Fluid Mechanics*, 32(1):709–778, 2000.

[5] W. E. Boyce, R. C. DiPrima, H. Villagómez Velázquez, et al. *Elementary differential equations and boundary value problems, 11th edition*. Wiley, 2017.

[6] R. Carnecky, T. Brunner, S. Born, J. Waser, C. Heine, and R. Peikert. Vortex Detection in 4D MRI Data: Using the Proper Orthogonal Decomposition for Improved Noise-Robustness. In N. Elmqvist, M. Hlawitschka, and J. Kennedy, editors, *EuroVis - Short Papers*. The Eurographics Association, 2014.

[7] M. S. Chong, A. E. Perry, and B. J. Cantwell. A general classification of three-dimensional flow fields. *Physics of Fluids A: Fluid Dynamics*, 2(5):765–777, 1990.

[8] M. Edmunds, R. S. Laramee, G. Chen, N. Max, E. Zhang, and C. Ware. Surface-based flow visualization. *Computers & Graphics*, 36(8):974–990, 2012.

[9] S. Farooq, M. Huarte-Espinosa, and R. Ostilla-Mónico. Large-scale structures in high-reynolds-number rotating waleffe flow. *Journal of Fluid Mechanics*, 884, Dec 2019.

[10] C. Garth, F. Gerhardt, X. Tricoche, and H. Hans. Efficient computation and visualization of coherent structures in fluid flow applications. *IEEE Transactions on Visualization and Computer Graphics*, 13(6):1464–1471, 2007.

[11] C. Garth, A. Wiebel, X. Tricoche, K. Joy, and G. Scheuermann. Lagrangian visualization of flow-embedded surface structures. *Computer Graphics Forum*, 27(3):1007–1014, 2008.

[12] M. Gavish and D. L. Donoho. The optimal hard threshold for singular values is $4/\sqrt{3}$. *IEEE Transactions on Information Theory*, 60(8):5040–5053, 2014.

[13] G. Gilka, D. Luchtenburg, F. Thiele, and M. Morzynski. Dynamic characterization of an actuated bluff body wake. 06 2010.

[14] T. Günther and H. Theisel. The state of the art in vortex extraction. *Computer Graphics Forum*, 37:149–173, 2018.

[15] H. Guo, W. He, T. Peterka, H. Shen, S. M. Collis, and J. J. Helmus. Finite-time lyapunov exponents and lagrangian coherent structures in uncertain unsteady flows. *IEEE Transactions on Visualization and Computer Graphics*, 22(6):1672–1682, 2016.

[16] J. H. Tu, C. W. Rowley, D. M. Luchtenburg, S. L. Brunton, and J. Nathan Kutz. On dynamic mode decomposition: Theory and applications. *Journal of Computational Dynamics*, 1(2):391–421, 2014.

[17] G. Haller. Lagrangian coherent structures and the rate of strain in two-dimensional turbulence. *Phys. Fluids A*, 13:3365–3385, 2001.

[18] G. Haller. An objective definition of a vortex. *Journal of Fluid Mechanics*, 525:1–26, 2005.

[19] G. Haller and G. Yuan. Lagrangian coherent structures and mixing in two-dimensional turbulence. *Physica D: Nonlinear Phenomena*, 147(3):352 – 370, 2000.

[20] J. C. Hunt, A. Wray, and P. Moin. Eddies, streams, and convergence zones in turbulent flows. In *Studying Turbulence Using Numerical Simulation Databases, 2*, volume 1, pages 193–208, 1988.

[21] M. R. Jovanović, P. J. Schmid, and J. W. Nichols. Sparsity-promoting dynamic mode decomposition. *Physics of Fluids*, 26(2):024103, Feb 2014.

[22] G. Kerschen, J.-c. Golinval, A. F. Vakakis, and L. A. Bergman. The method of proper orthogonal decomposition for dynamical characterization and order reduction of mechanical systems: An overview. *Nonlinear Dynamics*, 41(1):147–169, 2005.

[23] T. Krake, S. Reinhardt, M. Hlawatsch, B. Eberhardt, and D. Weiskopf. Visualization and selection of dynamic mode decomposition components for unsteady flow. *Visual Informatics*, 5(3):15–27, 2021.

[24] J. N. Kutz, S. L. Brunton, B. W. Brunton, and J. L. Proctor. *Dynamic Mode Decomposition: Data-Driven Modeling of Complex Systems*. Society for Industrial and Applied Mathematics, Philadelphia, PA, 2016.

[25] J. N. Kutz, X. Fu, and S. L. Brunton. Multi-resolution dynamic mode decomposition. *SIAM Journal on Applied Dynamical Systems*, 15(2):713–735, 2016.

[26] R. Laramee, H. Hauser, L. Zhao, and F. H. Post. Topology based flow visualization: the state of the art. In *Topology-Based Methods in Visualization (Proceedings of Topo-in-Vis 2005)*, Mathematics and Visualization, pages 1–19. Springer, 2007.

[27] J. Marston, G. Chini, and S. Tobias. Generalized quasilinear approximation: application to zonal jets. *Physical review letters*, 116(21):214501, 2016.

[28] P. J. S. Mihailo R. Jovanović and J. W. Nichols. Sparsity-promoting dynamic mode decomposition. *Physics of Fluids*, 26(2):024103, Feb 2014.

[29] D. B. Nguyen, R. O. Monico, and G. Chen. A visualization framework for multi-scale coherent structures in taylor-couette turbulence. *IEEE Transactions on Visualization and Computer Graphics*, Preprint:1–1, 2020.
[30] Nvidia. Cuda toolkit documentation. https://docs.nvidia.com/cuda/.
[31] R. Ostilla-Mónico, R. Verzicco, S. Grossmann, and D. Lohse. The near-wall region of highly turbulent taylor–couette flow. *Journal of Fluid Mechanics*, 788:95–117, 2016.
[32] R. Ostilla-Mónico, R. Verzicco, and D. Lohse. Effects of the computational domain size on direct numerical simulations of taylor-couette turbulence with stationary outer cylinder. *Physics of Fluids*, 27(2):025110, Feb 2015.
[33] G. Pascarella, I. Kokkinakis, and M. Fossati. Analysis of transition for a flow in a channel via reduced basis methods. *Fluids*, 4(4):202, 2019.
[34] R. Peikert and M. Roth. The "parallel vectors" operator-a vector field visualization primitive. In *Proceedings Visualization '99 (Cat. No.99CB37067)*, pages 263–532, Oct 1999.
[35] S. D. Pendergrass, J. N. Kutz, and S. L. Brunton. Streaming gpu singular value and dynamic mode decompositions, 2016.
[36] A. Pobitzer, R. Peikert, R. Fuchs, B. Schindler, A. Kuhn, H. Theisel, K. Matkovic, and H. Hauser. The state of the art in topology-based visualization of unsteady flow. *Computer Graphics Forum*, 30(6):1789–1811, September 2011.
[37] A. Pobitzer, M. Tutkun, Andreassen, R. Fuchs, R. Peikert, and H. Hauser. Energy-scale aware feature extraction for flow visualization. *Computer Graphics Forum*, 30(3):771–780, 2011.
[38] E. D. Robertson, Y. Wang, K. Pant, M. J. Grismer, and J. A. Camberos. A flow feature detection framework for large-scale computational data based on incremental proper orthogonal decomposition and data mining. *International Journal of Computational Fluid Dynamics*, 32(6-7):261–277, 2018.
[39] F. Sacco, R. Verzicco, and R. Ostilla-Mónico. Dynamics and evolution of turbulent Taylor rolls. *J. Fluid Mech.*, 870:970–987, 2019.
[40] I. A. Sadarjoen and F. H. Post. Geometric methods for vortex extraction. In *Data Visualization'99*, pages 53–62. Springer, 1999.
[41] I. A. Sadarjoen and F. H. Post. Detection, quantification, and tracking of vortices using streamline geometry. *Computers & Graphics*, 24(3):333–341, 2000.
[42] S. G. Saddoughi and S. V. Veeravalli. Local isotropy in turbulent boundary layers at high Reynolds number. *J. Fluid Mech.*, 268:333–372, 1994.
[43] F. Sadlo and R. Peikert. Efficient visualization of lagrangian coherent structures by filtered amr ridge extraction. *IEEE Transactions on Visualization and Computer Graphics*, 13(6):1456–1463, 2007.
[44] T. Salzbrunn, T. Wischgoll, H. Jänicke, and G. Scheuermann. The state of the art in flow visualization: Partition-based techniques. In H. Hauser, S. Strassburger, and H. Theisel, editors, *In Simulation and Visualization 2008 Proceedings*, pages 75–92. SCS Publishing House, 2008.
[45] T. Sayadi and P. J. Schmid. Parallel data-driven decomposition algorithm for large-scale datasets: with application to transitional boundary layers. *Theoretical and Computational Fluid Dynamics*, 30(5):415–428, 2016.
[46] P. J. Schmid. Dynamic mode decomposition of numerical and experimental data. *Journal of Fluid Mechanics*, 656(August):5–28, 2010.
[47] S. C. Shadden. *Lagrangian Coherent Structures*, chapter 3, pages 59–89. John Wiley Sons, Ltd, 2011.
[48] J. A. Sillero, J. Jiménez, and R. D. Moser. Two-point statistics for turbulent boundary layers and channels at reynolds numbers up to + 2000. *Physics of Fluids*, 26(10):105–109, 2014.
[49] S. H. Strogatz. *Nonlinear Dynamics And Chaos: With Applications To Physics, Biology, Chemistry, And Engineering*. CRC Press, 1 edition, 2000.
[50] H. L. Swinney and J. P. Gollub. *Hydrodynamic instabilities and the transition to turbulence*. Springer-Verlag, 1985.
[51] G. I. Taylor. Viii. stability of a viscous liquid contained between two rotating cylinders. *Philosophical Transactions of the Royal Society of London. Series A, Containing Papers of a Mathematical or Physical Character*, 223(605-615):289–343, 1923.
[52] S. Tobias and J. Marston. Three-dimensional rotating couette flow via the generalised quasilinear approximation. *Journal of Fluid Mechanics*, 810:412–428, 2017.
[53] M. Treib, K. Bürger, F. Reichl, C. Meneveau, A. Szalay, and R. Westermann. Turbulence visualization at the terascale on desktop pcs. *IEEE Transactions on Visualization and Computer Graphics*, 18(12):2169–2177, 2012.
[54] Y. Wang, J. Qian, H. Song, K. Pant, H. Q. Yang, X. Li, M. J. Grismer, J. A. Camberos, and F. Fahroo. Feature extraction from massive, dynamic computational data based on proper orthogonal decomposition and feature mining. *Journal of Visualization*, 17(4):363–372, Nov 2014.
[55] T. Weinkauf and H. Theisel. Streak lines as tangent curves of a derived vector field. *IEEE Transactions on Visualization and Computer Graphics*, 16(6):1225–1234, 2010.
[56] A. Wiebel, R. Chan, C. Wolf, A. Robitzki, A. Stevens, and G. Scheuermann. Topological flow structures in a mathematical model for rotation-mediated cell aggregation. In *Topological Methods in Data Analysis and Visualization*, pages 193–204. Springer, 2011.
[57] Z. Wu, D. Laurence, S. Utyuzhnikov, and I. Afgan. Proper orthogonal decomposition and dynamic mode decomposition of jet in channel crossflow. *Nuclear Engineering and Design*, 344:54–68, 2019.
[58] Q. Zhang, Y. Liu, and S. Wang. The identification of coherent structures using proper orthogonal decomposition and dynamic mode decomposition. *Journal of Fluids and Structures*, 49:53 – 72, 2014.

Duong B. Nguyen earned his Ph.D. in Computer Science from the Department of Computer Science, University of Houston in 2020. He received a BS in Information Technology from Vietnam National University, Ha Noi in 2012. His research interests include computer graphics, large-scale scientific data analysis and visualization.

Panruo Wu is an Assistant Professor of Computer Science at University of Houston. Prior to joining UH, he was a postdoc research with Innovative Computing Laboratory at University of Tennessee Knoxville. He earned his Ph.D. degree from University of California Riverside in 2016. His research interests include matrix/tensor computations and numerical optimizations at large scale and on accelerators.

Rodolfo Ostilla-Monico is an Assistant Professor at the Department of Mechanical Engineering, University of Houston. He earned a Ph.D. degree in the Physics of Fluids department at the University of Twente in 2015. His research interests include numerical simulations of convective flows, vortex ring colissions and more generally, of turbulent systems.

Guoning Chen is an Associate Professor at the Department of Computer Science at the University of Houston. He earned a Ph.D. degree in Computer Science from Oregon State University in 2009. His research interests include visualization, data analytics, computational topology, geometric modeling, geometry processing and physically-based simulation. He is a member of ACM and IEEE.